Pergamon

Geochimica et Cosmochimica Acta, Vol. 61, No. 21, pp. 4689–4704, 1997

0016-7037/97 $17.00 + .00

PII S0016-7037(97)00267-6

Formation and metamorphism of group A5 chondrules in ordinary chondrites

SHAOXIONG HUANG* and DEREK W. G. SEARS

Cosmochemistry Group, Department of Chemistry and Biochemistry, University of Arkansas, Fayetteville, Arkansas 72701, USA

(*Received February* 28, 1996; *accepted in revised form July* 10, 1997)

Abstract—Group A5 chondrules have FeO-rich olivines (>4 wt% FeO) and albite-normative mesostases and thus are discrete from the major primary chondrule groups. Group A5 chondrules in six LL chondrites have been studied by cathodoluminescence, optical microscopy, electron-micropobe, and, in the case of four chondrules removed from Semarkona (type 3.0) and Krymka (type 3.1), by instrumental neutron activation analysis. Olivine and pyroxene compositions vary with petrographic type in a manner resembling group B1 chondrules (they gain FeO and MnO, lose CaO, MgO, Al_2O_3, and Cr_2O_3 and become more homogeneous), but the pyroxene trends are less marked because of lower diffusion rates. There are no metamorphically-related compositional trends in the mesostasis, although compositional zoning is common in the mesostases of two type 3.4–3.7 chondrites. Group A5 chondrules contain unfractionated lithophile element bulk compositions but, as is typical of all chondrules, siderophile, and chalcophile elements are depleted by about an order of magnitude.

Group A5 chondrules are abundant in equilibrated (100% by number) but rare in unequilibrated ordinary chondrites (UOCs, 5% by number), but their presence in UOCs is not due to the emplacement of metamorphosed chondrules during brecciation because (1) olivine in group A5 chondrules is heterogeneous, (2) the olivine displays all the compositional properties of olivine in low petrographic type ordinary chondrites, and (3) the mesostasis is not recrystallized. The chondrules display trends that are consistent with chondrule-to-chondrule and chondrule-to-matrix mineral homogenization and equilibration during metamorphism. Like the major chondrule groups A1, A2, and B1 in Semarkona, group A5 is a primary group whose presence provides further insights into chondrule formation process and diversity. Their bulk composition and redox state suggest that the conditions and temperatures of formation for groups A5 and B1 were similar, however, their different mesostasis compositions indicate that their post-solidification histories were different. Either group B1 chondrules experienced slower cooling at low temperatures than group A5, during which albite crystallized in the mesostasis, group B1 suffered a subsequent mild reheating that caused albite crystallization in the mesostasis, or nucleation details for crystallization of albite in the residual melt were different. Group A1 and A2 chondrules could have been derived from group A5- or B1-like material by reduction and evaporative loss during chondrule formation. *Copyright © 1997 Elsevier Science Ltd*

1. INTRODUCTION

Chondrules are silicate beads present in many classes of meteorite. They arguably provide insights into the early solar system processes (Dodd, 1981; King, 1983; Hewins et al., 1996). However, theories for their origin are numerous and diverse, ranging from impact onto a planetary surface to a wide variety of nebular or even interstellar processes (Grossman, 1988; Boss, 1996).

Chondrules are highly diverse in their properties, and an important step in understanding their origin and history is their classification. Early chondrule classification schemes involved complex descriptions of texture (Dodd, 1978; Gooding and Keil, 1981), then several schemes were proposed that involved a mixture of texture and mineral composition (McSween, 1977a,b; McSween et al., 1983; Scott and Taylor, 1983), and most recently we have proposed a scheme involving only the compositions of the major phases (Sears et al., 1992, 1995b). Chondrule properties reflect both formation and subsequent metamorphism, either dry and at moderate to high temperatures (Dodd et al., 1967; McSween et al., 1988; Sears et al., 1980), or wet and at low temperatures (Hutchison et al., 1987). To complicate matters further, brecciation was widespread and may have caused disimilar material to become mixed making it essential to classify chondrules with a scheme that is independent of the host meteorite.

The compositional classification scheme for chondrules (Sears et al., 1992, 1995b; DeHart et al., 1992) was prompted by cathodoluminescence observations but is based on Ca-Fe plots for the olivine and normative albite, anorthite, and quartz plots for the chondrule mesostasis (Figs. 1 and 2). Eight chondrule classes are defined by these plots, four are present in the essentially unmetamorphosed Semarkona chondrite (A1, A2, A5, and B1, which can be considered as the primary groups), while four are only found in more metamorphosed chondrites (A3, A4, B2, B3, the secondary groups). The secondary groups are most probably produced from the primary groups as metamorphism drives the chondrules to a uniform composition consistent with the bulk composition of the host meteorite. Group A5 are unique in appearing in both equilibrated (petrographic types 4–6) and unequilibrated (petrographic types 3) chondrites, but while

* *Present address:* Conair Corporation, 205 Shellhouse Drive, Rantoul, Illinois 61866, USA.

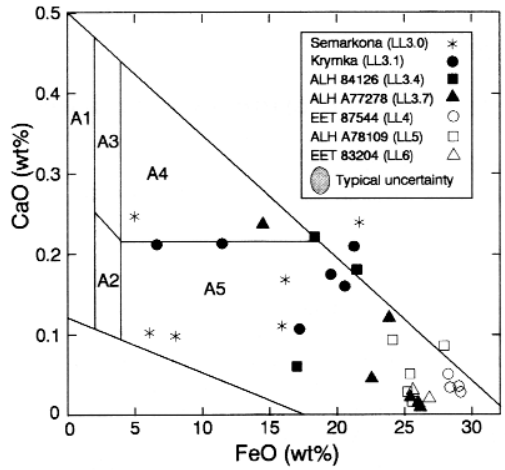

Fig. 1. Plot of CaO vs. FeO for olivines in group A5 chondrules from seven LL chondrites with the fields defining the compositional classes of chondrule indicated (Sears et al., 1995b; Huang et al., 1996). Through the petrologic type 3 series, CaO decreases and FeO increases until equilibrated values of <0.1 wt% CaO and 25–27 wt% FeO are reached. Within the types 4–6 these values remain constant.

they are of similar mean composition, group A5 chondrules in unequilibrated chondrites are more heterogeneous in composition. The compositional groups A1, A2, and B1 in Semarkona are essentially equivalent to the types IA, IAB, and II, etc. of McSween, Scott and others, but the equivalence breaks down for meteorites more metamorphosed than Semarkona. While roughly 30% of the chondrules in Semarkona are group A1 or A2, and 60% are group B1, only 5% are group A5. The equilibrated chondrites contain only group A5 chondrules (DeHart et al., 1992).

Group A5 chondrules are defined as those whose olivine contains >4 wt% FeO and whose mesostasis has 70–100% normative plagioclase with Ab >50 wt%. By comparison, group A1 and A2 chondrules have <4 wt% FeO in their olivine and anorthite-normative mesostases while group B1 chondrules have >4 wt% FeO and mesostases with considerable quartz in their norms (>50 wt% in Fig. 2). These compositional properties are reflected in major differences in CL, and this makes them easy to locate in large sections. While group A1 and A2 chondrules have mesostases with conspicuous yellow CL (the olivine grains having red CL in group A1 and are nonluminescent in group A2), and group B1 chondrules are nonluminescent, group A5 chondrules have an equally conspicuous blue CL, and the enclosed grains do not luminesce. When textures are fine, the CL data can be superior to electron microprobe data in assigning classes.

It is probable that group A1 and A2 chondrules formed from a similar mixture of precursor materials as group B1 but suffered considerable reduction and volatilization during formation. In contrast, group B1 chondrules suffered little reduction and evaporation (Huang et al., 1996). However, other authors have argued that the different classes simply reflect different mixes of precursor materials (e.g., Grossman and Wasson, 1983). Whether the diversity in chondrule properties is a reflection of compositional diversity in the precursors, or variations in the intensity or nature of the chondrule-forming process, or a combination of both, the identification of a new class of chondrule is important in constraining the process. The present paper represents the first attempt to describe and discuss the unique group A5 class of chondrules.

2. EXPERIMENTAL

2.1. Sample Selection

Sections of Semarkona (LL3.0, prepared by us from chips from USNM 1805), Krymka (LL3.1, AMNH 1729-1, 1729-9), ALH 84216 (LL3.4, PTS #15), ALH A77278 (LL3.7, PTS #27), EET 87544 (LL4, PTS #13), ALH A78109 (LL5, PTS #33), and EET 83204 (LL6, PTS #9) were used for the present study, the petrologic types being taken from Van Schmus and Wood (1967), Sears et al. (1980, 1991), or the appropriate issue of the Antarctic Meteorite Newsletter. Semarkona and Krymka belong to shock stages S2 and S3, respectively, of Stöffler et al. (1991), the shock classification of the remaining meteorites being undetermined. Our samples are all LL chondrites because only this class contains the full range of petrographic type. Although Semarkona is widely regarded as the least-metamorphosed ordinary chondrite (Sears et al., 1980; Huss et al., 1981), it shows evidence for mild levels of aqueous alteration in the matrix and a few chondrules (Hutchison et al., 1987, Sears et al., 1995a). Krymka is only slightly more metamorphosed than Semarkona (it is type 3.1). The remaining meteorites in this study are petrologic types 3.4–6. Many of our samples are from the Antarctic but show only minor signs of weathering. Allan Hills A77278 (LL3.7) is a breccia containing carbonaceous xenoliths (McSween

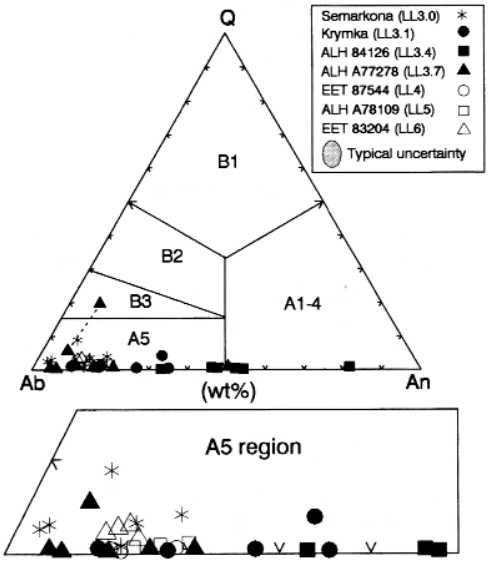

Fig. 2. Normative quartz, anorthite, and albite (wt%) for mesostasis compositions with the chondrule group fields indicated. Together with Fig. 1, this plot defines the eight compositional chondrules classes (Sears et al., 1995b; Huang et al., 1996). All meteorites in the present study plot in the A5 field with no indication of trends with petrologic type. ALH 84126 and ALHA77278 show unusually high degrees of heterogeneity. We suggest that this is because secondary A5 chondrules are being formed by metamorphism. The two data points for ALHA77278 connected by a tie line are an example of the compositional zoning in the mesostasis of group A5 chondrules in type 3.4–3.7 chondrites.

and Wilkening, 1980) and metal grains with a range of cooling rates (Scott et al., 1982).

2.2. Cathodoluminescence (CL)

Mosaics of the CL of entire sections were prepared using a commercial Luminoscope attached to a low-powered optical microscope (Smith and Stenstrom, 1965; Marshall, 1988; DeHart, 1989; Lu et al., 1990). As discussed above, their unique CL provides a means of rapidly searching large sections for the relatively rare A5 chondrules. Kodacolor Gold-400 film and 30–90 s exposures were used, the film being developed using the C-41 process.

2.3. Petrography

The texture of each chondrule was noted using the nomenclature of Gooding and Keil (1981). The apparent diameters of the chondrules were measured using the CL mosaics, averaging measurements in two perpendicular directions.

2.4. Instrumental Neutron Activation Analysis

Thick sections (1–2 mm) of Semarkona and Krymka were also prepared from material provided by the USNM and Michael Lipschutz and the A5 chondrules located by CL, removed by chiseling (using stainless steel dental tools), cleaned of adhering materials by scraping, and heat-sealed in high-density polyethylene vials for instrumental neutron activation analysis (INAA). The samples and standards were irradiated in a flux of 10^{14} neutrons $cm^{-2}s^{-1}$ at the University of Missouri Research Reactor for 3 min and then counted three times for 3 min to determine Mg, Al, V, and Ca, and then irradiated for 30 min and counted for 15 min, 2 h, 4 h, and 12 h over a six week period to determine Mn, Sc, Cr, Na, K, REE, Ir, Co, Ni, Fe, Au, As, Ga, Se, and Zn. The SPECTRA5 interactive computer program, which incorporates corrections for spectral interference and interactive manual placement of the baseline, was used for data reduction (Baedecker and Grossman, 1989). Our procedures were monitored using secondary standards (BCR-1 and an in-house Allende powder sample).

2.5. Electron-Microprobe Analysis

Backscattered electron imaging and wavelength-dispersive analysis of olivine, pyroxene, and mesostasis were performed on a Camebax electron microprobe at the Johnson Space Center (JSC) in Houston, using an accelerating voltage and sample current of 15 kV and 40 nA, respectively. Typical beam diameters were 1 μm for olivine and pyroxene (point mode) and 3 μm for mesostasis analyses (raster mode). Microlites were avoided during the analysis of mesostasis because (1) it is often difficult to distinguish between silicate grains and microlites whereas pure glassy or microlite-free mesostasis is easily recognized and (2) the mesostasis CL properties that distinguish the chondrule classes are really those of the glassy or microlite-free mesostasis. Counting times were 15–50 s depending on the abundance and volatility of the elements being determined. Typical detection limits (in wt%) were: SiO_2, 0.03; TiO_2, Al_2O_3, and MgO: 0.02–0.03; FeO, MnO, and Cr_2O_3: 0.03–0.04; Na_2O and K_2O: 0.01–0.02. Four Semarkona chondrules (SC-12-4, SC-12-14, SC-14-4, and SC-16-9) were analyzed at the American Museum of Natural History using an ARL-SEMQ electron microprobe (Huang et al., 1996). Olivine and mesostasis compositions were determined in virtually all of the chondrules studied, and pyroxene was present and was analysed in just over half of them. Four to six silicate grains and four to six regions of the mesostasis were analyzed for each chondrule. Bulk compositions were determined for four Semarkona chondrules using a defocused electron beam, metal and sulfide being excluded from the analyses because of their heterogeneity and low abundance.

3. RESULTS

3.1. Chondrule Classes and Abundance

As expected, the present A5 chondrules selected on the basis of their CL plot in the group A5 fields of Figs. 1 and 2. Only one mesostasis point for ALH 84126 plots significantly outside the A5 field, and this may reflect beam overlap with silicate grains. The mesostasis in ALH A77278 is compositionally zoned and at the center of the chondrule has B3 composition, a fairly common property of type 3.7 chondrites (DeHart et al., 1992).

The relative abundance of group A5 chondrules in the present meteorites as a function of petrographic type (Fig. 3) is very similar to that observed for an independent suite of type 3 ordinary chondrites discussed by Sears et al. (1995b).

3.2. Petrography

3.2.1. Semarkona (LL3.0) and Krymka (LL3.1)

The group A5 chondrules in these meteorites are circular to irregular in cross-section and have apparent diameters of

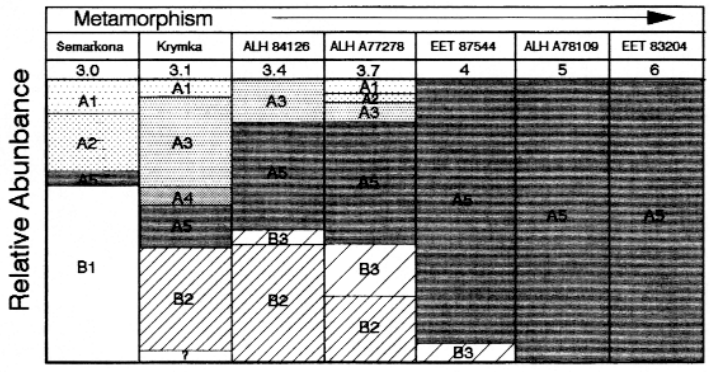

Fig. 3. The relative abundance of group A5 chondrules in the present samples compared with the other compositional classes. With increasing metamorphism, the number of group A5 chondrules increases, while the number in other classes decreases, so that by type 4 most of the chondrules in ordinary chondrites are group A5. For the purposes of this figure, where a rapid survey was required, chondrule classes were assigned on the basis of their cathodoluminescence properties (DeHart et al., 1992).

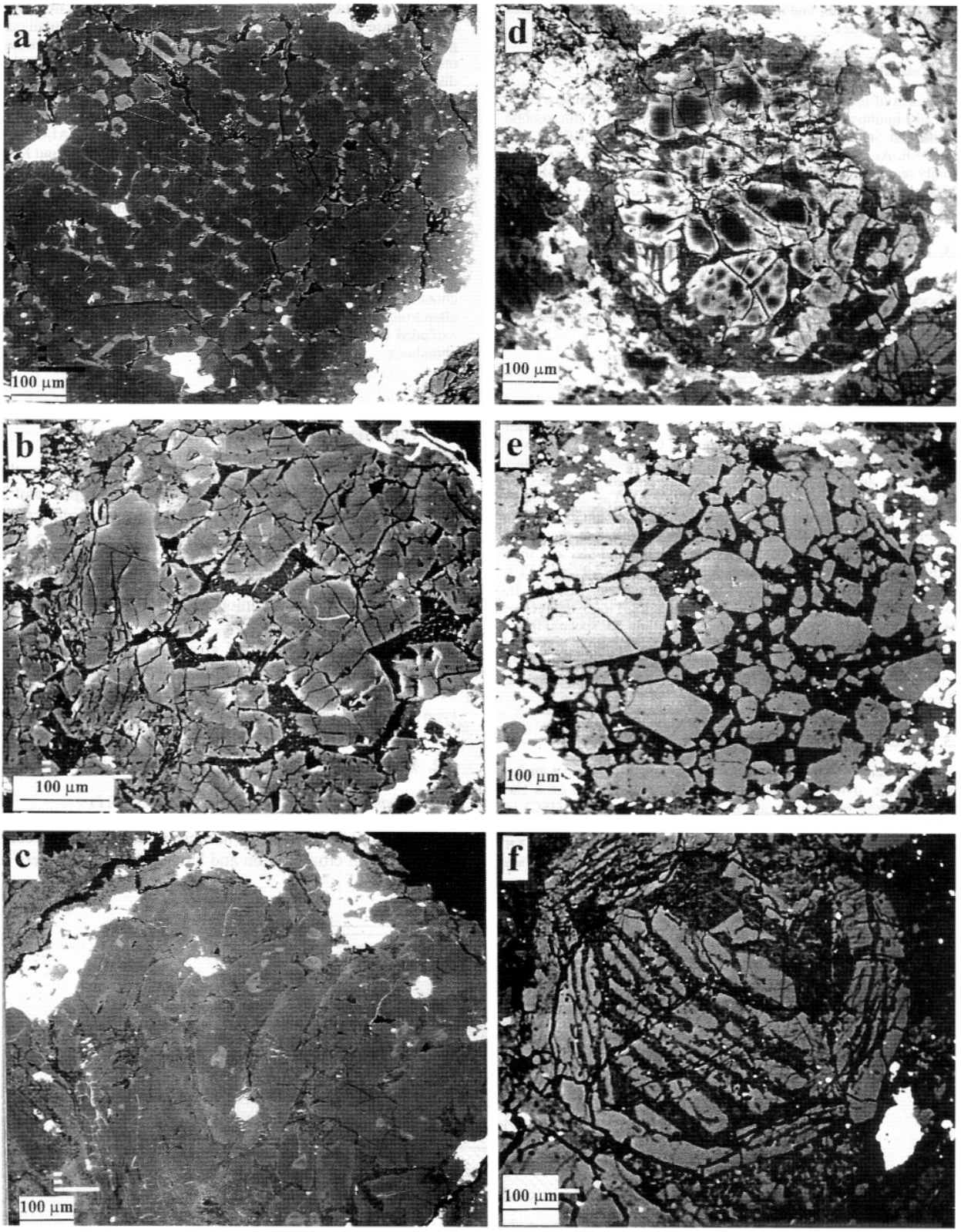

Fig. 4. Backscattered electron images of group A5 chondrules in LL ordinary chondrites. Major phases include olivine and pyroxene phenocrysts (gray), and mesostasis (dark gray), except for Fig. 4a, where the refractory mesostasis is lighter than olivine and pyroxene phenocrysts. (a) Semarkona (LL3.0), (b) Krymka (LL3.1), (c) ALH 84126 (LL3.4), (d) ALH A77278 (LL3.7), (e) EET 87544 (LL4), and (f) ALH A78109 (LL5). While group A5

220–3300 mm with means of 774 ± 452 mm (Semarkona) and 707 ± 255 mm (Krymka). Most are porphyritic-olivine or porphyritic-olivine-pyroxene chondrules. Olivine is euhedral to subeuhedral grain sizes of a few μm to a few hundred μm. They often show resorption at the edges (Fig. 4a). Uniform backscattered electron (BSE) images reflect a lack of FeO and MgO zoning (Fig. 4a,b). Some olivines contain mesostasis regions of various sizes and shapes. Low-Ca pyroxene grains are common near chondrule rims and often enclose olivine. Some chondrules contain orthopyroxene with exsolution lamellae of clinopyroxene typically a few mm in width. Both olivine and pyroxene grains show well-formed crystal faces in contact with mesostasis. The chondrules normally contain <1 wt% of metal and sulfide.

About one third of the A5 chondrules in Semarkona are completely or partially rimmed with fine-grained material. Like the matrix, the chondrule rims display a distinctive red CL (which we suspect is due to the presence of submicrometer forsterite grains) and contain finely dispersed or massive sulfides and metal.

3.2.2. *The LL3.4-LL6 chondrules*

The size distribution of the group A5 chondrules in the higher types is the same as for Semarkona and Krymka (apparent diameter 360–2010 μm with a mean of 822 ± 312 μm and no significant difference between meteorites). All textural types are found (porphyritic-olivine, porphyritic-olivine-pyroxene, granular, radiating-pyroxene, and barred-olivine) although some textures might dominate in certain meteorites.

ALH 84126 (LL3.4) contains many chondrule fragments, some of which contain compositionally zoned grains (Fa_{12-20}, Fs_{6-16}, Fig. 4c). ALH A77278 (LL3.7) contains abundant chondrules with olivines that are sometimes strongly zoned (Fa_{8-20}, Fig. 4d), and contain polysynthetically twinned clinopyroxene. ALH 84126 and ALHA77278 mesostases are glassy or microcrystalline and sometimes show CL zoning, with the margin showing blue CL while the core is nonluminescent. The chondrules in EET 87544 (LL4) are mostly group A5 with compositionally zoned olivines (Fig. 4e). The mesostases are sometimes partially recrystallized. ALH A78109 (LL5) contains abundant chondrules, some broken or deformed, with small grains of plagioclase in the mesostases (Fig. 4f). The chondrules in EET 83204 (LL6) are weakly defined, only two were located in the present section, and contain extensively recrystallized mesostasis.

3.3. Phase Analysis

3.3.1. *Olivine*

Olivine compositions are given in Table 1. Fayalite in A5 chondrules is ~10 times group A1 values and ~2 times group A2 values and comparable with group B1 values but increases with petrographic type. As expected, MnO correlates with FeO in group A5 olivines (Fig. 5), albeit poorly ($r^2 = 0.48$), and MgO, Al_2O_3, CaO, and Cr_2O_3 decrease with petrographic type. Olivine heterogeneity also varies with petrographic type, with Semarkona A5 chondrules showing the widest range (for example, FeO, 6.3–22.9 wt%, CaO 0.10–0.26 wt%) and chondrules in equilibrated chondrules having the smallest range (FeO 24.2–28.5 wt%), CaO 0.02–0.05 wt%).

Compositional zoning in the olivines of group A5 chondrules is shown in Fig. 6. In general, the zoning increases with the petrographic type of the host meteorite. For Semarkona, the zoning is generally weak (Fig. 6a), and BSE images confirm this is not universal, while Krymka A5 olivines show stronger zoning (Fig. 6b). ALH 84126 (LL3.4) resembles Semarkona (Fig. 6c). Some group A5 chondrule olivines in ALHA77278 show little zoning (Fig. 6d) while others enrichments of FeO and MnO and depletions of CaO (Fig. 6e). In EET 87544, FeO is homogeneous, while MnO is slightly enriched in CaO (and possible Cr_2O_3) are slightly depleted at the rim (Fig. 6f).

3.3.2. *Pyroxene*

Most pyroxenes in group A5 chondrules are low in CaO (Table 1). FeO, MgO, and Cr_2O_3 show trends with petrographic type similar to those of olivine and TiO_2 increases with metamorphism, but Al_2O_3 and MnO do not. There is a weak ($r^2 = 0.56$) positive correlation between CaO and FeO (Fig. 7). A zoning profile was obtained for ALH 84126 chondrule pyroxene (Fig. 8). FeO, CaO, TiO_2, and Al_2O_3 show enrichments at the rim, while Cr_2O_3 is depleted at the rim and MnO is essentially unzoned.

3.3.3. *Mesostasis*

Our compositions for A5 chondrule mesostases are given in Table 1 and plotted in Fig. 2. The mesostases are generally depleted in CaO and enriched in Na_2O (~6%) relative to group A1,2. Group A5 mesostases are poor in SiO_2 relative to those of group B1. The mesostases of group A5 chondrules are scattered in composition with no clear trends with petrologic type, TiO_2 excepted. TiO_2 concentration in the mesostases tends to decrease with increasing petrologic type. Compositional zoning of the mesostasis was common in ALHA77278 and present in ALH 84126, so that the central regions show purple CL, the outer region show blue CL, the central region have compositions of B3 chondrules, and the outer regions have composition of A5 chondrules. These regions are connected with tie-lines in Fig. 2.

chondrules are most frequently porphyritic in texture, with phenocrysts that appear light in these images surrounded by darker mesostasis, group A5 chondrules can exist with any texture. Most olivine/pyroxene grains in Semarkona are not zoned, but in several cases (especially in chondrites of petrologic types 3.4–3.7) compositional zoning is apparent in these images as a lightening towards the rim. Many, but not all group A5 chondrules, are surrounded by a rim of fine-grained material that is enriched in sulfide and metal, the sulfide and metal appearing white in these images.

Table 1. Mean olivine, pyroxene, and mesostasis compositions (wt% oxide) for group A5 chondrules.[†]

	N	SiO_2	TiO_2	Al_2O_3	Cr_2O_3	FeO	MnO	MgO	CaO	Na_2O	K_2O	Total
Olivine												
Semarkona	6	39.7 ± 1.0	0.02 ± 0.01	0.10 ± 0.07	0.51 ± 0.16	12.6 ± 6.5	0.65 ± 0.38	45.5 ± 5.6	0.17 ± 0.06	—	—	99.2
Krymka	7	38.6 ± 1.4	0.02 ± 0.01	0.18 ± 0.12	0.23 ± 0.14	16.4 ± 5.0	0.32 ± 0.17	42.6 ± 4.2	0.19 ± 0.04	—	—	98.5
ALH 84126	4	38.5 ± 0.8	0.01 ± 0.02	0.12 ± 0.10	0.10 ± 0.08	21.3 ± 4.3	0.39 ± 0.07	39.7 ± 3.8	0.14 ± 0.07	—	—	100.3
ALH A77278	7	37.2 ± 0.6	0.03 ± 0.02	0.08 ± 0.05	0.10 ± 0.08	25.1 ± 1.2	0.45 ± 0.02	36.3 ± 1.2	0.04 ± 0.03	—	—	99.3
EET 87544	4	36.6 ± 0.4	0.01 ± 0.01	0.02 ± 0.02	0.01 ± 0.01	28.5 ± 0.4	0.45 ± 0.01	34.5 ± 0.2	0.04 ± 0.01	—	—	100.1
ALH A78109	4	36.8 ± 1.0	0.01 ± 0.01	0.14 ± 0.15	0.02 ± 0.01	25.1 ± 0.5	0.46 ± 0.01	36.6 ± 1.4	0.05 ± 0.01	—	—	99.2
EET 83204	2	36.4 ± 1.1	0.02 ± 0.01	0.02 ± 0.02	0.02 ± 0.01	26.1 ± 0.7	0.45 ± 0.01	35.0 ± 0.9	0.02 ± 0.01	—	—	98.2
AI[‡]	8	41.4 ± 0.4	0.05 ± 0.02	0.31 ± 0.17	0.24 ± 0.12	0.65 ± 0.12	0.18 ± 0.16	56.9 ± 0.7	0.37 ± 0.09	—	—	100.1
A2[‡]	3	41.2 ± 0.3	—	—	0.45 ± 0.12	2.47 ± 0.81	0.21 ± 0.11	55.4 ± 0.1	0.16 ± 0.01	—	—	99.9
B1[‡]	3	40.0 ± 0.4	—	—	0.44 ± 0.05	11.0 ± 1.2	0.48 ± 0.15	48.1 ± 1.0	0.12 ± 0.04	—	—	100.1
Pyroxene												
Semarkona	6	56.8 ± 1.9	0.06 ± 0.02	0.58 ± 0.31	0.84 ± 0.15	7.9 ± 3.6	0.55 ± 0.19	32.1 ± 3.1	0.80 ± 0.51	—	—	99.6
Krymka	4	56.5 ± 1.3	0.04 ± 0.01	0.33 ± 0.10	0.75 ± 0.15	8.7 ± 4.5	0.45 ± 0.06	32.1 ± 3.2	0.42 ± 0.28	—	—	99.3
ALH 84126	3	55.9 ± 1.9	0.06 ± 0.01	0.60 ± 0.07	0.61 ± 0.12	9.3 ± 2.8	0.41 ± 0.05	31.3 ± 2.5	0.59 ± 0.44	—	—	98.8
ALH A77278	2	55.1 ± 1.0	0.08 ± 0.05	1.03 ± 0.66	0.57 ± 0.04	12.1 ± 6.0	0.38 ± 0.15	28.4 ± 3.9	1.16 ± 0.06	—	—	98.8
ALH A78109	1	54.9	0.16	0.17	0.17	15.1	0.45	28.1	0.80	—	—	99.9
EET 83204	2	54.5 ± 0.1	0.20 ± 0.01	0.39 ± 0.19	0.16 ± 0.04	15.8 ± 0.1	0.46 ± 0.02	27.1 ± 0.2	1.19 ± 0.28	—	—	99.8
AI[‡]	6	57.6 ± 1.2	0.25 ± 0.10	2.31 ± 1.17	0.73 ± 0.18	0.80 ± 0.35	0.29 ± 0.13	35.3 ± 1.9	2.32 ± 1.33	—	—	99.6
A2[‡]	6	58.0 ± 0.4	0.09 ± 0.04	0.80 ± 0.48	0.79 ± 0.23	2.43 ± 1.2	0.47 ± 0.40	36.9 ± 2.2	0.47 ± 0.64	—	—	100.0
B1[‡]	2	57.8 ± 0.9	0.03 ± 0.02	0.21 ± 0.03	0.57 ± 0.08	5.12 ± 2.8	0.35 ± 0.09	34.7 ± 1.8	0.35 ± 0.03	—	—	99.1
Mesostasis												
Semarkoma	6	64.0 ± 2.6	0.39 ± 0.12	16.0 ± 2.2	0.09 ± 0.09	3.9 ± 1.0	0.13 ± 0.04	3.1 ± 2.3	4.0 ± 2.0	7.7 ± 1.4	0.17 ± 0.05	99.5
Krymka	4	56.9 ± 2.1	0.36 ± 0.13	17.3 ± 6.5	0.29 ± 0.31	6.2 ± 2.3	0.21 ± 0.08	7.0 ± 8.0	5.5 ± 1.9	5.6 ± 1.8	0.22 ± 0.28	99.6
ALH 84126	6	52.8 ± 2.2	0.38 ± 0.18	24.5 ± 5.0	0.15 ± 0.08	4.1 ± 2.6	0.33 ± 0.21	2.7 ± 1.7	10.3 ± 2.9	4.6 ± 1.2	0.09 ± 0.03	100.0
ALH A77278	6	57.5 ± 4.4	0.41 ± 0.10	13.8 ± 3.0	0.52 ± 0.31	4.4 ± 1.6	0.16 ± 0.05	7.9 ± 2.1	8.2 ± 2.4	5.4 ± 1.0	1.01 ± 0.70	99.3
EET 87544	4	56.0 ± 0.71	0.23 ± 0.10	9.17 ± 1.9	0.49 ± 0.18	5.3 ± 2.5	0.14 ± 0.02	10.5 ± 0.9	12.3 ± 3.5	4.1 ± 0.8	0.63 ± 0.60	98.9
ALH A78109	3	57.0 ± 1.1	0.16 ± 0.05	11.9 ± 2.4	0.21 ± 0.10	5.4 ± 2.5	0.14 ± 0.07	11.1 ± 3.0	8.2 ± 3.7	5.3 ± 1.5	0.48 ± 0.08	99.9
EET 83204	2	64.5 ± 1.2	0.06 ± 0.01	21.4 ± 0.6	0.05 ± 0.06	1.0 ± 1.1	0.02 ± 0.02	0.6 ± 1.0	2.3 ± 0.2	9.4 ± 0.3	0.63 ± 0.08	100.0
AI[‡]	8	52.4 ± 3.9	0.77 ± 0.27	22.6 ± 3.1	—	1.3 ± 1.0	—	5.5 ± 1.3	16.6 ± 2.0	1.0 ± 0.9	0.03 ± 0.14	100.2
A2[‡]	6	53.4 ± 5.2	0.50 ± 0.10	20.4 ± 2.6	—	3.0 ± 0.8	—	5.4 ± 1.5	9.9 ± 1.8	4.0 ± 1.5	0.18 ± 0.06	96.8
B1[‡]	4	69.4 ± 3.5	0.53 ± 0.07	14.0 ± 1.4	—	5.8 ± 1.6	—	1.8 ± 0.8	4.7 ± 3.9	2.1 ± 0.9	0.74 ± 0.22	99.1

[†] "*N*" refers to number of chondrules. The errors refer to 1σ uncertainties on the mean.
[‡] Huang et al. (1996).

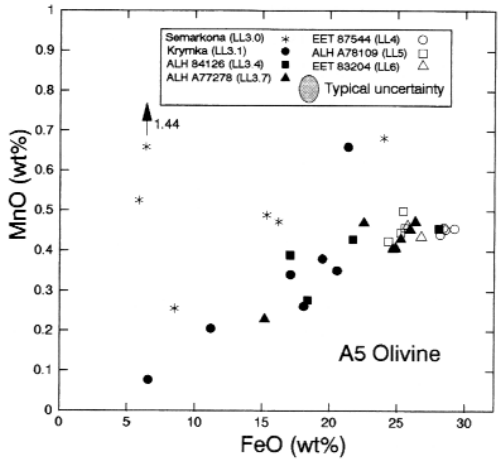

Fig. 5. A plot of MnO vs. FeO in chondrule olivine ($r^2 = 0.48$). The concentration of both these cations increases with metamorphism until they reach values of 0.4–0.5 wt% MnO and 25–27 wt% FeO. Two Semarkona chondrules contain extremely high MnO, which we attribute to the heterogeneity of their precursors. As with CaO and FeO, A5 chondrules in meteorites of petrologic types 4–6 are uniform in MnO and FeO.

3.3.4. Bulk compositions

Analysis by defocused electron microprobe and INAA yield similar results (Table 2), allowing for sample heterogeneity and the analytical uncertainty. (The low thermal neutron cross section for Ca means that INAA values carry large uncertainties.) The INAA data are plotted in Fig. 9, along with literature data for Hamlet and Soko-Banja A5 chondrules (Gooding, 1979), normalized to Mg and CI, and arranged in order of increasing volatility within cosmochemical affinity. The lithophile element abundance patterns are essentially flat (i.e., element ratios are CI-like), in contrast to those of groups A1 and A2, which show volatility-related elemental abundance patterns, and like those of group B1 chondrules. Siderophiles and chalcophiles show the order of magnitude depletions common to all chondrules.

4. DISCUSSION

4.1. Primary and Secondary A5 Chondrules

Most (perhaps all) chondrites are breccias, containing a wide variety of fragments showing various degrees of metamorphism (Binns, 1968; Keil, 1982). Dodd (1968, 1971, 1974) and Scott (1984) found that some type 3 ordinary chondrites contain individual equilibrated chondrules and

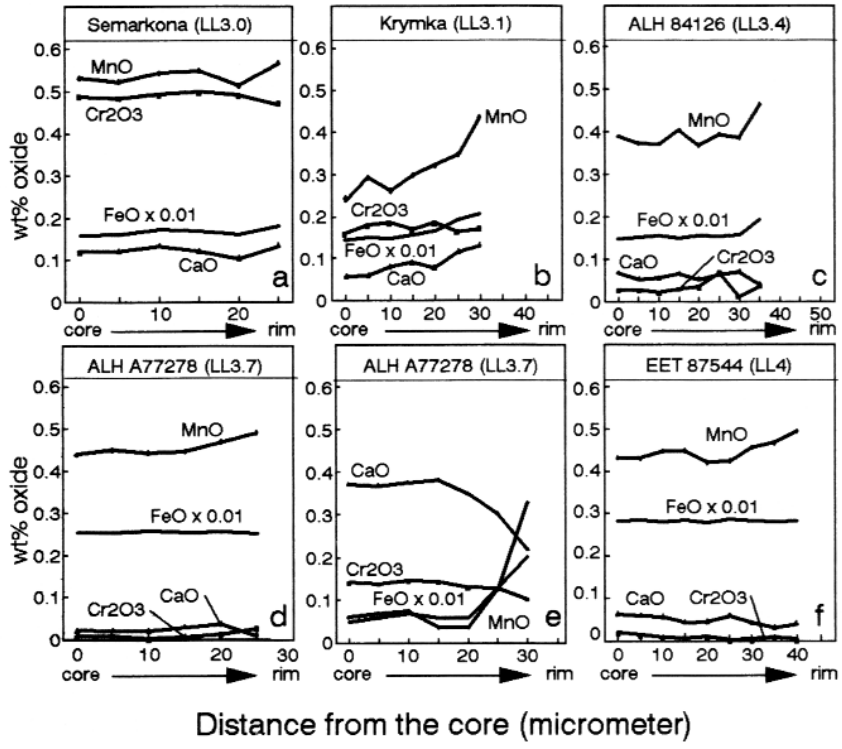

Fig. 6. Compositional profiles in the olivine of group A5 chondrules. One chondrule in ALH A77278 (3.7) is strongly zoned, where MnO and FeO increase and CaO and Cr_2O_3 decrease towards the rim, reflecting diffusive equilibration between olivine and other components in the meteorite. Zoning profiles for other chondrules are similar but are generally weaker.

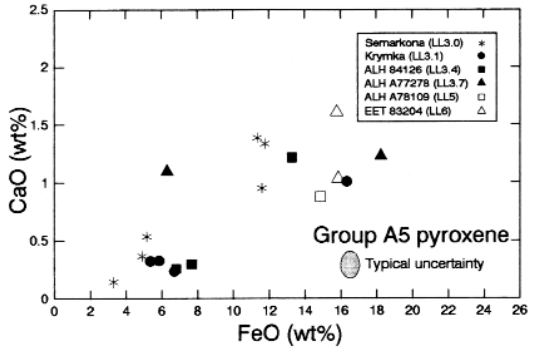

Fig. 7. Plot of CaO vs. FeO in the low-Ca pyroxene of group A5 chondrules ($r^2 = 0.56$). Concentrations of these elements increase with increasing petrologic type until they reach the equilibrated values of ~1.5 wt% CaO and ~16–18 wt% FeO.

concluded that metamorphic equilibration must have occurred before assembly of the present chondrite. Armstrong et al. (1982) and Meeker et al. (1983) made a similar suggestion to explain some of the diversity in CAI structures, mineralogy, and oxygen isotopes. Since only 5% of the chondrules in Semarkona are group A5 and 100% of the chondrules in equilibrated chondrites are group A5, it is at least arguable that the A5 chondrules in low petrologic type chondrites are interlopers from equilibrated chondrites. However, the components of group A5 chondrites in low petrologic type chondrites are compositionally more heterogeneous than group A5 chondrites in the higher petrographic type chondrites (see Fig. 10 and discussion below). It is difficult to see how metamorphism could have changed the composition of a the major phases in a chondrule from those of a group A1, A2, or B1 to those of A5 without homogenizing their composition. In addition, the recrystallized chondrules discussed by Dodd (1968, 1971, 1974) contain <0.05 wt% Ca, (similar to the equilibrated chondrites in the present study) whereas the group A5 chondrules in Semarkona (and Krymka) contain >0.1 wt% CaO (Fig. 1). Apparently, in addition to making highly reduced and refractory compositions and chondrules whose mesostasis is Si-rich, the chondrule-forming process was capable of producing chondrules with bulk and phase compositions resembling those of equilibrated chondrules.

4.2. Metamorphism of A5 Chondrules

Metamorphism resulted in the recrystallization of mineral grains, blurring of chondritic texture, devitrification of glass, and formation of secondary feldspar. The textural differences among type 3–6 appear to result largely from the progressive thermal metamorphism of material that originally resembled type 3 chondrites (Van Schmus and Wood, 1967; Dodd, 1969; Sears and Hasan, 1987; McCoy et al., 1991). Group A5 chondrules display all these effects.

Mineralogical changes due to metamorphism are similar to those of group B1 chondrules, as chondrule-to-chondrule and chondrule-to-matrix diffusive exchange occurred (Huss et al., 1981; Lux et al., 1980; McCoy et al., 1991; Sears et al., 1992; DeHart et al., 1992). Olivine shows a decrease in CaO, MgO, Al_2O_3, and Cr_2O_3 and an increase in FeO and possibly MnO with increasing metamorphism, while TiO_2 is constant.

The heterogeneity (expressed as the coefficient of variation of FeO in olivine, σ/Fa) increases from 1–16% in Semarkona and Krymka, to 5–16% in ALH 84126 (LL3.4), and 1–44% in ALH A77278 (LL3.7), then decreases to <4% in EET 87544 (LL4) and <2% in ALH A78109 (LL5). The pyroxenes in general show an increase in CaO and FeO with petrologic type, so that there is a positive correlation (Fig. 7, Table 1). The increase in heterogeneity from type 3.0–3.4 is consistent with an initial population which is being made even more heterogeneous as metamorphism converts other groups into group A5.

Miyomoto et al. (1986) described several types of compositional profile in the olivine of chondrules from type 3 chondrites, including primary igneous profiles and secondary metamorphic profiles. The profiles observed in the present samples (Fig. 6) are consistent with metamorphically-induced diffusion of FeO and MnO into the grains and Cr_2O_3 and CaO, the steepness of the gradients being determined by diffusion rates (Morioka, 1981). The diffusion profiles of MgO, FeO, and Cr_2O_3 in pyroxene are similar to those in olivine (e.g., Fig. 8), although diffusion rates are generally lower, except that TiO_2 gradients increase slowly with metamorphism, and Al_2O_3 and MnO show no trends.

Compositions of mesostases in A5 chondrules do not show marked trends, except for TiO_2, which decreases through type 4–6. The concentration of Fe decreases with petrologic type, consistent with the increase in FeO in the olivine and pyroxene (Table 1). These metamorphic trends have been often described in the literature, but there has been little or no discussion of compositionally zoned chondrule mesostasis. Matsunami et al. (1993) described a particularly large group A1

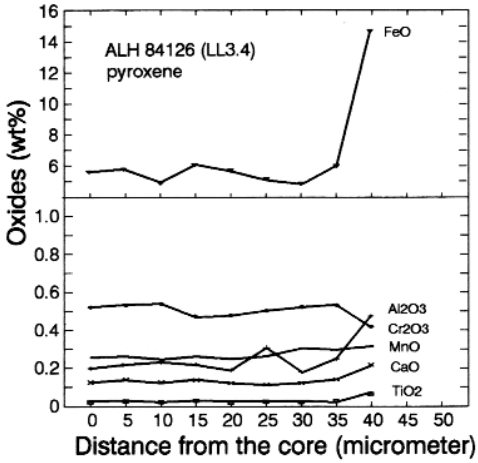

Fig. 8. Compositional profiles in the low-Ca pyroxene of the ALH 84126 (LL3.4) ordinary chondrite. The profiles are fairly flat except that FeO increases steeply towards the rim. Al_2O_3, TiO_2, and CaO show modest increases towards the rim while Cr_2O_3 decreases.

Table 2. Bulk compositions of group A5 chondrules.

Electron-microprobe defocused beam analysis (wt %)

	N[†]	SiO_2	TiO_2	Al_2O_3	Cr_2O_3	FeO	MnO	MgO	CaO	Na_2O	K_2O	Total
Semarkona A5	4	45.6	0.16	2.82	0.62	12.53	0.65	35.4	2.13	0.65	0.09	100.7
1σ		2.8	0.09	1.71	0.31	4.32	0.19	10.0	1.69	0.29	0.05	
A1[‡]	8	45.1	0.19	5.34	0.42	2.14	0.16	42.6	3.31	0.33	0.03	99.6
A2[‡]	5	54.8	0.15	3.74	0.83	3.95	0.47	32.5	2.43	0.44	0.04	99.3
B1[‡]	5	49.7	0.07	1.52	0.63	11.70	0.65	34.0	1.11	0.48	0.09	100.0

Instrumental neutron activation analysis (lithophile elements)

	Al mg/g	Ca mg/g	Sc μg/g	La ng/g	Sm ng/g	Yb ng/g	Lu ng/g	V μg/g	Mg mg/g	Cr mg/g	Mn mg/g	Na mg/g	K mg/g
Semarkona A5	—	12.0	6.7	310	340	330	42	64	170	3.49	4.06	6.44	0.60
Krymka A5	14	13	7.8	—	260	—	—	100	158	2.68	2.26	8.45	1.18
Hamlet A5[§]	16	16	11.5	410	310	390	46	97	163	4.43	2.62	8.47	—
Soko-Banja A5[§]	13	17	10.1	290	220	220	31	83	160	4.42	3.87	8.33	—
A1[‡]	—	14	10.3	300	220	290	38	65	133	2.69	1.20	3.47	0.36
A2[‡]	—	14	6.0	320	220	300	64	70	121	2.86	1.78	3.77	0.31
B1[‡]	—	13	8.2	270	218	270	45	63	122	3.45	2.81	6.42	1.06

Instrumental neutron activation analysis (siderophile and chalcophile elements).

	Ir ng/g	Co μg/g	Ni mg/g	Fe mg/g	Au ng/g	As μg/g	Ga μg/g	Se μg/g	Zn μg/g
Semarkona A5	172	213	4.80	107	63.3	0.79	2.4	11	20
Krymka A5	67	111	2.22	107	—	—	2.6	—	—
Hamlet A5[§]	231	131	3.61	117	52	—	—	—	39
Soko-Banja A5[§]	91	94	1.37	140	35	—	—	—	46
A1[‡]	267	405	8.31	143	55	0.99	3.2	4.89	57
A2[‡]	269	334	6.86	110	72	1.35	3.7	12.9	69
B1[‡]	319	205	6.72	126	75	0.72	4.2	5.02	39

[†] "N" refers to number of chondrules. The errors refer to 1σ uncertainties on the mean.
[‡] Huang et al. (1996).
[§] Gooding (1979).

chondrule in Semarkona, and they ascribed zoning in its mesostasis to Na entering the refractory chondrule from the outside, such as would be expected if Na recondensed on the surface of the chondrule. The observation was subsequently confirmed by Grossman (1996) who suggested that the Na was being redistributed by aqueous means, but this is unlikely because of analytical sums are close to 100% whereas aqueously altered mesostasis invariably have low sums (Hutchison et al., 1987). Additionally, aqueous alteration during low-temperature hydrothermal annealing experiments destroys the CL of chondrule mesostasis (DeHart and Lofgren, 1996). The present observations of zoned mesostasis in the A5 chondrules of type 3.4–3.7 chondrites differ from the Semarkona observations in their ubiquity, perhaps 30% of the chondrule mesostasis in ALHA77214 are compositionally zoned (DeHart et al., 1992). We suggest that for these higher petrographic type meteorites metamorphism caused both internal homogenization as essentially closed-systems and equilibration through diffusive exchange with matrix and other chondrules as open-systems. Thus the composition of the outer zone can always be derived by processes equivalent to metamorphism of the inner zone. It is as if the metamorphism of an individual chondrule had been trapped halfway.

4.3. Formation of Primary Group A5 Chondrules

Chondrules of all classes cooled rapidly (they have essentially quench textures) and show evidence for major disequilibrium between the composition of the silicate grains and the mesostasis. Since compositional zoning in Semarkona and Krymka olivines in A5 chondrules is limited (Fig. 6a,b), it is possible to use the average olivine/pyroxene and mesostasis compositions to calculate the approximate partition coefficients (Table 3). The values for Ca and Al in olivine and low-Ca pyroxene are of similar magnitude to the equilibrium values determined by Colson et al. (1988) and Dunn (1987). Values for MnO and Cr_2O_3 are generally higher than the literature equilibrium values (Akella et al., 1976; Dunn, 1987; Colson et al., 1988). Values for Ti are higher in olivine and lower in pyroxene than equilibrium values taken from the literature (Dunn, 1987). K_D values $((FeO/MgO)_{olivine}/(FeO/MgO)_{liquid})$ scatter between 0.03 and 2.15, but are generally smaller than the equilibrium value of 0.3 (Roeder and Emslie, 1970), suggesting that equilibrium was not achieved during crystallization of group A5 chondrules. The departure from equilibrium values of Ti, Mn, Cr, and K_D is probably due to fast cooling. The lack of compositional zoning in

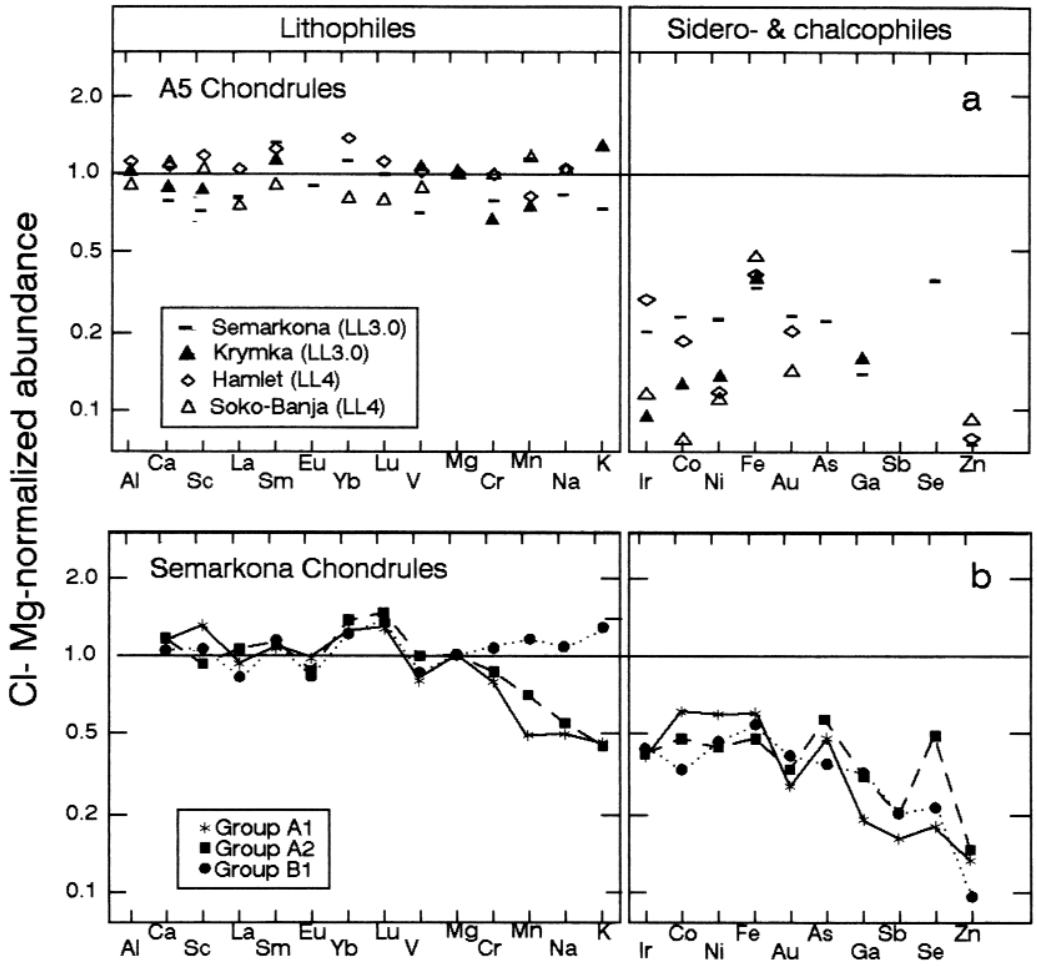

Fig. 9. Bulk compositions determined by instrumental neutron activation analysis for (a) A5 chondrules in different petrologic types and (b) major chondrule groups in Semarkona. In Fig. 9a, lithophile elements show flat (i.e., CI-like) abundances regardless of the petrologic type of the host meteorite, like those of the group B1 chondrules in Fig. 9b, while siderophiles and chalcophile elements are depleted by 50–90%. Data for Semarkona and Krymka A5 chondrules are from the present work, while data for Hamlet and Soko Banja are from Gooding (1979) and the group A1, A2, and B1 means are from Huang et al. (1996).

Smemarkona olivine suggests that Semarkona cooled relatively slowly, 30°C/h or less (Miyamoto et al., 1986). Lofgren found that group A5 starting compositions cooled at 100°C/h yielded stronger profiles than those of Semarkona A5 chondrules, consistent with a cooling rate slower than this (see Jones, 1990). Semarkona group A5 chondrules share many textural features with group A1 chondrules (e.g., olivines sometimes show resorption at the grain edges, and pyroxene often poikilitically encloses olivine) and may have cooled at similar rates. DeHart and Lofgren (1996) recently reproduced the texture and composition of group A1 chondrules with cooling rates of ~10°C/h.

There are major differences in the composition of the mesostases of group A1, A2, A5, and B1 chondrules that might also signal differences in crystallization sequence, as well as bulk composition (Fig. 11). While most chondrules plot in the olivine field, group A2 chondrules are close to the enstatite field, and group A1 chondrules are displaced to higher Al_2O_3. In an equilibrium crystallization sequence, melts with forsteritic compositions will first crystallize olivine, and the olivine will react with the melt to form pyroxene. However, instead of mesostasis compositions lying along the reaction line between olivine and protoenstatite fields, they plot in the mullilite field of Fig. 11. Apparently, none of the chondrules, including group A5, crystallized at equilibrium. Kimura and Yagi (1980) made similar observations for Yamato 74191 (L3) chondrules. The mesostases compositions actually plot in two clusters, one corresponding to groups A5 and B1 and one corresponding to groups A1 and A2 chondrules. These clusters are readily understood in terms of the bulk compositions of the various chondrule groups discussed by Huang et al. (1996). For groups A5 and B1, with unfractionated bulk compositions, the liquid compositions lie on line *X* passing through Fo and their bulk

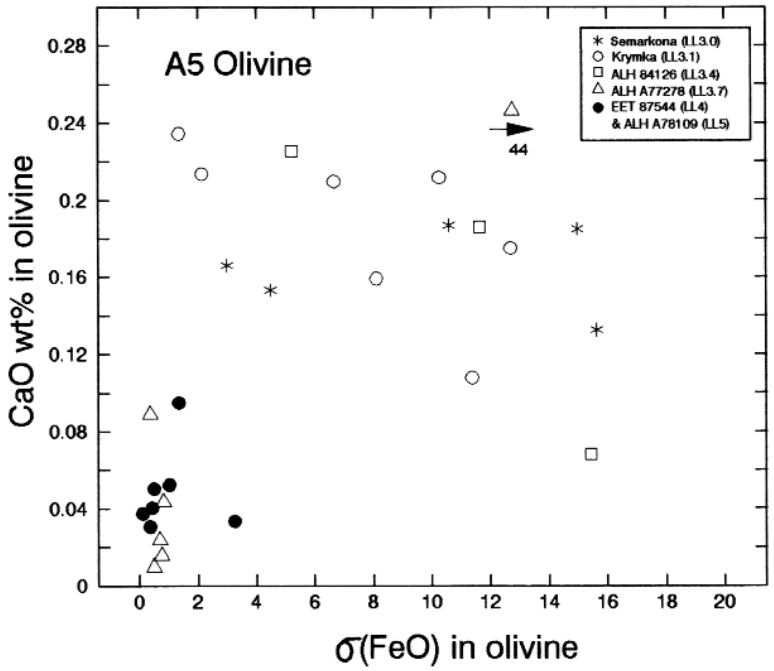

Fig. 10. CaO content of olivines in group A5 chondrules compared with compositional heterogeneity of the olivine measured as the σ(FeO) as a percent of the mean. Low types scatter widely, but have high CaO and σ(FeO) whereas high types have low CaO and σ(FeO).

compositions. The equivalent line for group A1 chondrules (line *Y*) is displaced to more Al_2O_3-rich compositions reflecting the bulk composition of group A1 chondrules is Al_2O_3-rich. Loss of FeO during chondrule formation resulted in a higher pyroxene to olivine ratios for group A2 chondrules, so the relevant section (line *Z*) is almost horizontal and passes through En and A2 bulk compositions. Thus all chondrules are nonequilibrium crystallization systems. The compositions of the mesostases are highly sensitive indicators of bulk compositions because bulk compositions are close to the MgO and SiO_2 axis of Fig. 11.

The compositional differences of the mesostasis are best observed using a plot CaO against Na_2O (Fig. 12). Group A1, A2, and A5 chondrules plot close to the stoichiometry of 70–100% plagioclase, with group A5 differing from the others in being Na-rich. Group B1 chondrules plot well-removed from plagioclase stoichiometry reflecting their quartz normative compositions (Fig. 2). In contrast to the other groups, group B1 chondrules show strong compositional zoning of FeO and minor elements, abundant dendritic microcrystallites in mesostasis; they are essentially pyroxene free, and olivine phenocrysts and quartz-normative mesostasis coexist (Jones, 1990; Huang et al., 1996).

The mesostasis of groups A5 and B1 are very different in composition despite their having similar unfractionated lithophile element bulk compositions. The explanation, at least partly, must lie in the ubiquitous microlites of group B1 chondrules, which are apparently Na-rich (Sears et al., 1995b). The abundance of Na-rich microlites in group B1 chondrules would signal major differences in the thermal histories of group B1 and A5 chondrules: perhaps the group B1 chondrules experienced two-stage cooling, so that they cooled more slowly at lower temperatures than group A5 chondrules, or perhaps group B1 chondrules experienced a subsequent heating event that group A5 chondrules missed. Another possibility is that the formation of microlytes is associated with faster cooling rates and supercooling for B1 chondrules. In a supercooled system, forsterite can not react with the residual liquid because of pyroxene nucleation difficulties, and quartz, higher than normative amounts of forsterite and no enstatite, are formed (Blander et al., 1976). This is obviously not the case in Semarkona group A1, A2, or A5 chondrules, where pyroxene is present.

The lack of significant elemental fractionation of the moderately volatile elements (Si, Cr, Mn, Na, and K) is important because Na-loss is rapid under a wide variety of experimental conditions (Gooding and Muenow, 1977; Tsuchiyama et al., 1981; Radomsky and Hewins, 1990). Volatile-loss from a molten droplet depends on temperature, bulk composition, oxygen fugacity, cooling rate, and droplet size. The Tsuchiyama et al. (1981) data for Na-loss are compared with the expected Fa for the olivine calculated from the Robie et al. (1979) thermodynamic tables in Fig. 13. Superimposed on the curves are the chondrule groups (Huang et al., 1996), including group A5. It is clear that chondrule formation was not an equilibirum process, but the temperatures deduced from Fig. 13 are in reasonable agreement with liquidus temperatures calculated from bulk compositions (Herzberg, 1979) suggesting that this approach is not entirely meaningless. Mean temperatures are ~1640°C for group A5, compared

Table 3. Apparent olivine/melt and pyroxene/melt partition coefficients.

Ol/melt	D (Ti)	D (Al)	D (Cr)	D (Mn)	D (Ca)	K_D
Semarkona						
SC-12-4	—	—	—	—	0.033	0.041
SC-12-14	—	0.007	—	—	0.055	0.21
SC-14-4	—	—	—	—	0.021	0.031
SC-16-9	—	—	—	—	0.034	2.15
SC-5-2	0.085	0.000	—	5.3	0.197	0.064
SC-5-5	0.017	0.011	2.455	2.8	0.044	0.33
Krymka						
KR-5-2	0.042	0.017	2.2	1.5	0.023	0.18
KR-5-5	0.046	0.023	0.18	1.6	0.062	1.24
KR-5-6	0.029	0.002	0.64	2.3	0.029	0.16
KR-5-14	0.004	0.002	1.3	4.3	0.022	0.29
Colson†	—	0.003	—	0.71	0.014	—
Colson‡	—	0.009	—	1.3	0.06	—
Dunn§	0.017	0.015	—	1.4	0.034	—
Akella¶	—	—	0.85	—	—	—
Roeder*	—	—	—	—	—	0.33

Px/melt	D (Ti)	D (Al)	D (Cr)	D (Mn)	D (Ca)
Semarkona					
SC-12-4	0.078	0.007	—	—	0.04
SC-12-14	0.33	0.034	—	—	0.068
SC-14-4	0.18	0.022	—	—	0.11
SC-5-2	0.16	0.038	—	5.7	1.6
SC-5-5	0.12	0.037	4.5	3.4	0.32
Krymka					
KR-5-5	0.068	0.046	0.73	1.9	0.11
Colson†	—	0.031	—	0.41	0.03
Colson‡	—	0.33	—	1.08	0.12
Dunn§	0.40	—	—	0.86	—

† Colson et al. (1988) (l).
‡ Colson et al. (1988) (h)
§ Dunn (1987).
¶ Akella et al. (1976).
* Roeder & Emslie (1970).

with ~1740°C, ~1570°C, and ~1630°C, for A1, A2, and B1, respectively (Huang et al., 1996). (Of course, if any of the chondrule groups were only partially melted, these numbers would be overestimates.) Oxygen fugacities were clearly many orders of magnitude higher than the nominal cosmic values required to prevent Na-loss, and a variety of mechanisms have been proposed: increasing the dust/gas ratio (Wood, 1985; Wood et al., 1989; Kitamura and Tsuchiyama, 1990; Hewins, 1991) and very rapid cooling (Connolly et al., 1993; Yu and Hewins, 1994).

An additional possibility is that Na may have been totally lost during chondrule formation, but reentered the chondrule as it cooled. Lewis et al. (1993) have found experimentally that in the presence of Na-rich vapor ($\sim 10^{-6}$ atm), Na is retained or even enriched in the sample under even high temperatures and low-oxygen fugacities. The Na-rich zones in chondrule mesostases discussed above suggest that some chondrules may have experienced this process.

4.4. Relationship to Other Chondrule Groups?

Like group B1 chondrules, group A5 chondrules are in general larger than group A1,2 chondrules, with group A1,2 chondrules typically having diameters about 85% of those of group A5 chondrules (Fig. 14). This amounts to a difference in mass of 40%, assuming uniform densities. The difference in mean diameter is significant at the 99.9% confidence level, according to the t-test. We have previously suggested that group A1,2 chondrules may have formed from group B1-like precursors by reduction and evaporation of FeO, SiO_2, and other volatiles (Huang et al., 1996), as opposed to variations among chondrule precursors (Grossman and Wasson, 1983; Grossman, 1988; Hewins, 1991; Jones, 1994). There is a general correlation between volatile abundance and size (Fig. 14), and it now appears that the precursor might also have had A5-like properties. This is not a surprising conclusion since the bulk compositions of group A5 and B1 chondrules are similar, except for some minor and trace elements, although they are quite different in terms of their phase compositions.

To test this idea, we performed the same simple mass-balance calculation that we previously reported for group B1 chondrules (Huang et al., 1996). A two-step process using thermodynamically reasonable estimates for element volatility (e.g., Hashimoto, 1983) readily explains the mass and compositional differences among group A5 and A1,2 chondrules in Semarkona (Table 4). Reduction of 90% of the FeO and evaporation of 90% of the Fe followed by evaporative loss of 30% of the SiO_2, and 10% of the MgO results in A1 composition and size relative to the group A5 chondrules. For group A2 chondrules, reduction of 80% of the FeO and evaporation of 90% of this followed by evaporative loss of 20% of the SiO_2, and 10% of the MgO is required. The agreement between the calculated mass losses and the observed mass differences would be better if a correction were made for differences in starting composition between the Hashimoto (1983) experiments and that of group A5 chondrules. In any event, this is a very oversimplified approach, since many factors, such as recondensation of volatiles (Matsunami et al., 1993), have been neglected. Nevertheless, these calculations suggest that chondrules in Semarkona may have formed from similar precursor materials by similar processes acting with different intensities, rather than from different precursors.

5. SUMMARY AND CONCLUSIONS

Group A5 chondrules are one of the four primary chondrule groups occurring in the essentially unmetamorphosed Semarkona chondrite, the others being groups A1, A2, and B1. Group A5 chondrules have olivine compositions resembling those of group B1 chondrules, and unlike the FeO-poor compositions (<4 wt%) of olivines from group A1 and A2 chondrules, they undergo compositional changes with metamorphism similar group B1 olivines. Group A5 chondrules contain a mesostasis which resembles that of group A1 and A2, albeit Na-rich rather than Ca-rich, whereas group B1 chondrules contain a mesostasis whose norms are quartz-rich and plagioclase-poor (<50 wt% in the norm). The bulk

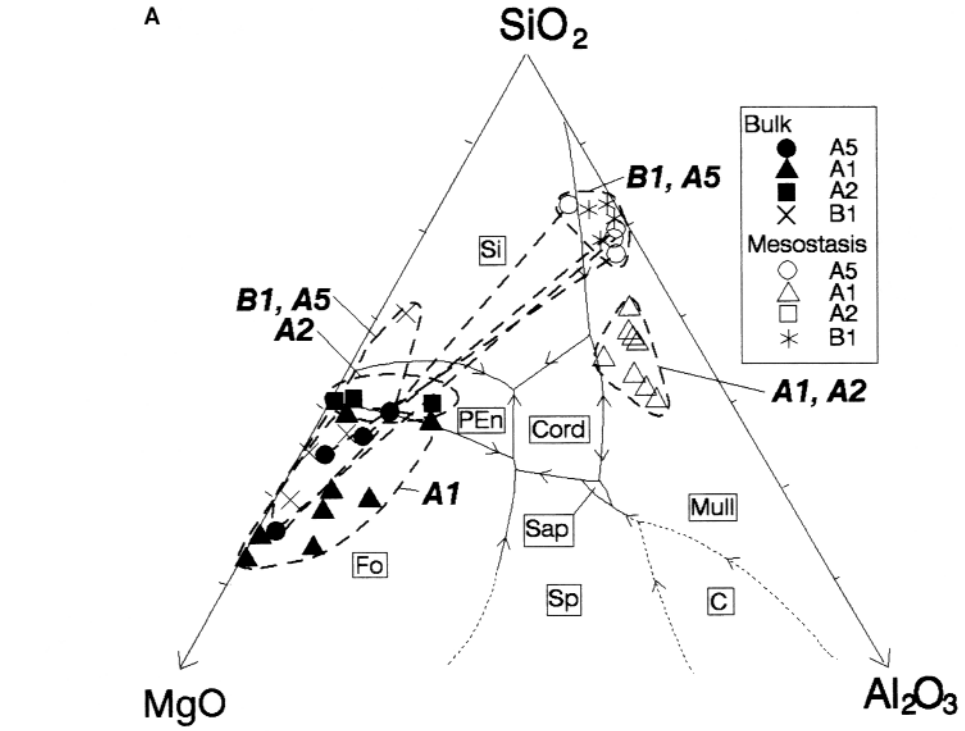

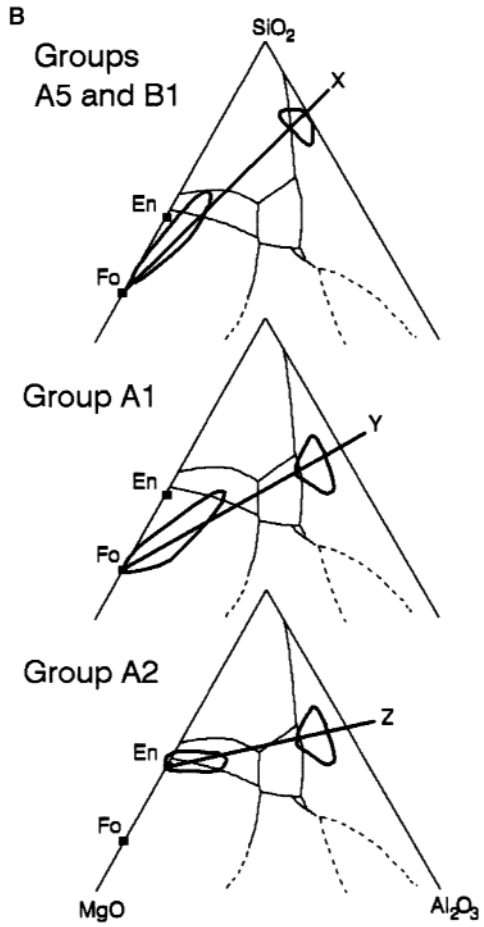

Fig. 11. (a) Bulk and mesostasis compositions for Semarkona chondrules plotted on part of the SiO_2-MgO-Al_2O_3 system of Muan and Osborn (1965). Si, silica; Pen, protoenstatite; Cord, cordierite; Mull, mullite; Fo, forsterite; Sp, spinel; Sap, saphorine; C, corundum. (b) Relationship between bulk composiiton and mesostasis composition explained as a failure to crystallize under equilibrium conditions, probably as a result of fast cooling, and with extrapolations to SiO_2-Al_2O_3-rich compositions as a result of inhibition of pyroxene or SiO_2 nucleation.

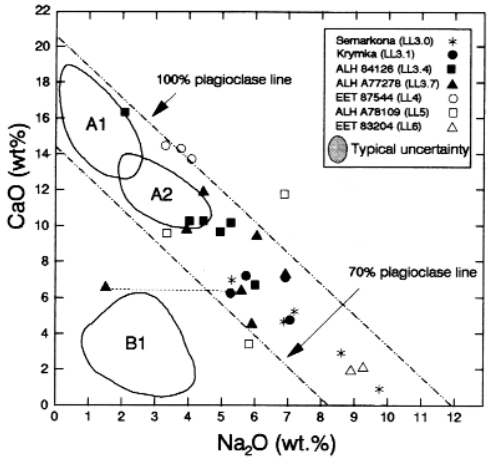

Fig. 12. Plot of CaO vs. Na_2O for chondrule mesostasis with the compositional classes indicated (DeHart et al., 1992). Group A5 chondrules generally plot between the 70 and 100% normative plagioclase lines with higher Na2O than group A1 and A2 chondrules and well-removed from group B1 chondrules which are mainly SiO_2-normative.

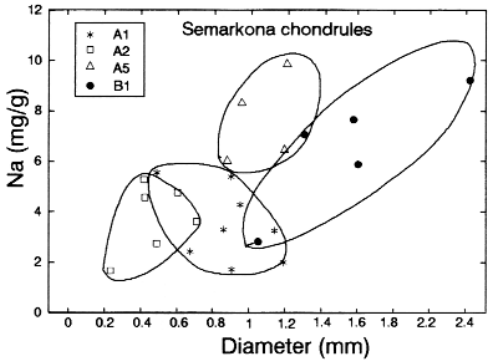

Fig. 14. Sodium vs. diameter for groups A5, A1, A2, and B1 chondrules. The four groups define a positive correlation between Na and size, suggesting that mass loss may have produced the size differences.

composition of group A5 chondrules resembles that of group B1 chondrules in having unfractionated lithophile element abundances but contrasts with groups A1 and A2 which show marked volatile element depletions. These mineral and phases compositions give group A5 chondrules unique cathodoluminescence properties which make the chondrules (which are rare in Semarkona, 5% by number) easy to find in thin sections. Group A5 chondrules are generally smaller than group B1 chondrules and at the upper end of the A1-A2 size range.

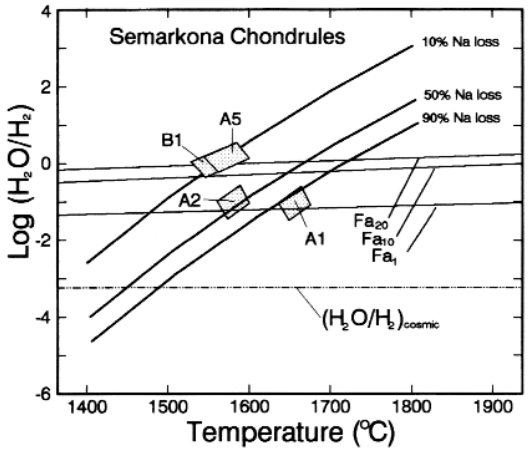

Fig. 13. Evaporation temperatures of chondrules as a function of oxygen fugacity (expressed as H_2O/H_2). Sodium loss from chondrule-like glass spheres is determined by the experiments of Tsuchiyama et al. (1981) and FeO reduction determined from equilibrium thermodynamic data (Robie et al., 1979; JANAF tables), with the fields appropriate to the chondrule groups superimposed. Cosmic H_2O/H_2 ratio is also indicated (data from Anders and Grevesse, 1989). Group A5 chondrules have bulk Na and FeO in olivine similar to group B1 chondrules equivalent to $f(O_2)$ values about 10^3 times higher than the cosmic value and temperatures comparable to group A2 and ~100°C below group A1. Data for group A1, A2, and B1 chondrules are from Huang et al. (1996).

The major conclusions of our study are: (1) Group A5 chondrules are not simply xenolithic objects from equilibrated chondrites because their olivine is compositionally more heterogeneous than olivine in equilibrated chondrules, and the mesostasis is not recrystallized. The olivine in these chondrules shows all the compositional changes with metamorphism observed for olivine in group B1 chondrules. Apparently, this is a new class of primary chondrule with the potential to provide additional information on the chondrule formation process and its diversity. (2) Group A5 chondrules probably experienced similar conditions and peak temperatures during chondrule formation as group B1, because their redox state and bulk composition are similar. Similar problems exist to those previously discussed in connection with group B1 chondrules in explaining the lack of volatile (particularly Na) loss in group A5 chondrules. (3) However, mesostasis compositions suggest important differences in crystallization and cooling history for group A5 and B1 chondrules. None of the chondrule groups display equilibrium between mesostasis and the large olivine and pyroxene grains, consistent with textures suggesting fast cooling and cooling rate estimates of 10–100°C/h. However, group B1 is unique in not containing plagioclase-normative mesostasis because, we suggest, plagioclase microlites have crystallized leaving a quartz-normative mesostasis. Either group A5 chondrules cooled more rapidly than group B1 chondrules following crystallization of the phenocrysts, so that albite microlites could not crystallize in group A5 chondrule mesostasis, group B1 chondrule underwent a secondary heating event during which the microlites crystallized, or nucleation details were different for the two classes.

Table 4. Derivation of group A1,2 chondrules from group A5 chondrules by reduction and evaporation of major elements (wt%) to give the observed sizes.*

	A5 Obs.	Step 1[&] Calc.	Step 2[&] Calc.	A1[¶] Calc.	A1[$] Obs.	Step 1[#] Calc.	Step 2[#] Calc.	A2[¶] Calc.	A2[$] Obs.
SiO_2	46	46	32	45	44	46	37	48	54
MgO	34	34	31	43	42	34	31	40	33
FeO	13	1.3	1.3	1.8	2.1	2.6	2.6	3.4	4.0
Al_2O_3	3.6	3.6	3.6	5.0	5.1	3.6	3.6	4.7	3.7
CaO	2.4	2.4	2.4	3.3	3.2	2.4	2.4	3.1	2.4
Fe (metal)	0	1.2	1.2	1.6	3.4	1.0	1.0	1.4	1.0
Diameter (mm)	0.77			0.69	0.65			0.71	0.67
Mass loss (wt%)	11	17		28		9	13	22	

* Relative mass loses are estimated from the experimental data of Hashimoto (1983) assuming 1700°C heating and 35–40% total mass loss, which corresponds to the mass differences between group A5 and A1,2 chondrules.

[&] Step 1, 90% of FeO is reduced, then 90% of the reduced Fe is evaporated; step 2, 30% of SiO_2, and 10% of MgO, is evaporated.

[#] Step 1, 80% of FeO is reduced, then 90% of the reduced Fe is evaporated; step 2, 20% of SiO_2, and 10% of MgO, is evaporated.

[¶] Previous column recalculated to 100%.

[$] Huang et al. (1996).

Acknowledgments—The authors are grateful to Vincent Yang and Dave McKay for use and technical assistance of electron microprobe analysis. We also wish to thank the Meteorite Working Group and Martin Prinz for supplying samples used in this study, Jeff Grossman for providing SPECTRA5 for INAA data reduction, Walter Manger for loan of the cathodoluminescence apparatus, Jerome Rose for use of his laboratory, and Steven Symes for technical assistance. This work is funded by NASA grant NAGW-3519.

Editorial handling: G. Faure

REFERENCES

Akella J., Williams R. J., and Mullins O. (1976) Solubility of chromium, titanium, and aluminum in coexisting olivine, spinel, and liquid at 1 atmosphere. *Proc. 7th Lunar Sci. Conf.,* 1179–1194.

Anders E. and Grevesse N. (1989) Abundance of elements: Meteoritic and solar. *Geochim. Cosmochim. Acta* **53,** 197–214.

Armstrong J. T., Meeker G. P., Huneke J. C., and Wasserburg G. J. (1982) The Blue Angel: I. The mineralogy and petrogensis of a hibonite inclusion from the Murchison meteorite. *Geochim. Cosmochim. Acta* **46,** 575–595.

Baedecker P. A. and Grossman J. N. (1989) The computer analysis of high resolution gamma-ray spectra from instrumental activation analysis experiments. *U. S. Geological Survey Open Report,* 89–454.

Binns R. A. (1968) Cognate xenoliths in chondritic meteorites: Examples in Mezö-Madaras and Ghubara. *Geochim. Cosmochim. Acta* **32,** 299–317.

Blander M., Planner H. N., Keil K., Nelson L. S., and Richardson N. L. (1976) The origin of chondrules: experimental investigation of metastable liquids in the system Mg2SiO2-SiO2. *Geochim. Cosmochim. Acta* **40,** 889–896.

Boss A. P. (1996) A concise guide to chondrule formation models. In *Chondrules and the Protoplanetary Disk* (ed. T. H. Hewins et al.), pp. 257–263. Cambridge Univ. Press.

Colson R. O., McKay G. A., and Taylor L. A. (1988) Temperature and composition dependencies of trace element partitioning: olivine/melt and low-Ca pyroxene/melt. *Geochim. Cosmochim. Acta* **52,** 539–553.

Connolly H. C., Jr., Hewins R. H., and Lofgren G. E. (1993) Flash melting of chondrule precursors in excess of 1600°C. Series I: Type II (B1) chondrule composition experiments. *Lunar Planet. Sci.* **XXIV,** 329–330.

DeHart J. M. (1989) Cathodoluminescence and Microprobe Studies of the unequilibrated Ordinary Chondrites. Ph.D. thesis, Univ. Arkansas.

DeHart J. M. and Lofgren G. E. (1996) Experimental studies of group A1 chondrules. *Geochim. Cosmochim. Acta* **60,** 2233–2242.

DeHart J. M., Lofgren G. E., Lu J., Benoit P. H., and Sears D. W. G. (1992) Chemical and physical studies of chondrules X: Cathodoluminescence studies of metamorphism and nebular processes in type 3 ordinary chondrites. *Geochim. Cosmochim. Acta* **56,** 3791–3807.

Dodd R. T. (1968) Recrystallized chondrules in the Sharp (H-3) chondrite. *Geochim. Cosmochim. Acta* **32,** 1111–1120.

Dodd R. T. (1969) Metamorphism of the ordinary chondrites: A review. *Geochim. Cosmochim. Acta* **33,** 161–203.

Dodd R. T. (1971) The petrology of chondrules in the Sharp meteorite. *Contrib. Mineral. Petrol.* **31,** 201–227.

Dodd R. T. (1974) The petrology of chondrules in the Hallingeberg Meteorite. *Contrib. Mineral. Petrol.* **47,** 97–112.

Dodd R. T. (1978) Compositions of droplet chondrules in the Manych (L3) chondrite and the origin of chondrules. *Earth Planet. Sci. Lett.* **40,** 71–82.

Dodd R. T. (1981) *Meteoritics, a Petrologic-Chemical Synthesis.* Cambridge Univ. Press.

Dodd R. T., Van Schmus R. T., and Koffman D. M. (1967) A survey of the unequilibrated chondrites. *Geochim. Cosmochim. Acta* **31,** 921–951.

Dunn T. (1987) Partitioning of hafnium, lutetium, titanium, and manganese between olivine, clinopyroxene, and basaltic liquid. *Contrib. Mineral. Petrol.* **96,** 476–484.

Gooding J. L. (1979) Petrogenetic properties of chondrules in unequilibrated H-, L-, and LL-group chondritic meteorites. Ph.D. thesis, Univ. New Mexico.

Gooding J. L. and Keil K. (1981) Relative abundances of chondrule primary textural types in ordinary chondrites and their bearing on conditions of chondrules formation. *Meteoritics* **16,** 17–43.

Gooding J. L. and Muenow D. W. (1977) Experimental vaporization of Holdrook chondrite. *Meteoritics* **12,** 401–408.

Grossman J. N. (1988) Formation of chondrules. In *Meteorites and the Early Solar System* (ed. J. F. Kerridge and M. S. Matthews), pp. 680–696. Univ. Arizona Press.

Grossman J. N. (1996) The redistribution of sodium in Semarkona chondrules by secondary processes. *Lunar Planet. Sci.* **XXVII,** 467–468.

Grossman J. N. and Wasson J. T. (1983) Refractory precursor components of Semarkona chondrules and the fractionation of refractory elements among chondrites. *Geochim. Cosmochim. Acta* **47,** 759–771.

Hashimoto A. (1983) Evaporation metamorphism in the early solar nebula-evaporation experiments on the melt FeO-MgO-SiO_2-CaO-Al_2O_3 and chemical fractions of primitive material. *Geochim. J.* **17,** 111–145.

Herzberg C. T. (1979) The solubility of olivine in basaltic liquids: an ionic model. *Geochim. Cosmochim. Acta* **43,** 1241–1251.

Hewins R. H. (1989) The evolution of chondrules. *Proc. 15th Symp. Antarctic Met.* **2,** 200–220.

Hewins R. H. (1991) Retention of sodium during chondrule formation. *Geochim. Cosmochim. Acta* **55,** 935–942.

Hewins T. H., Jones R. H., and Scott E. R. D., eds. (1996) *Chondrules and the Protoplanetary Disk.* Cambridge Univ. Press.

Huang S., Lu J., Prinz M., Weisberg M. K., Benoit P. H., and Sears D. W. G. (1996) Chondrules: Their diversity and the role of open-system processes during their formation. *Icarus* **122,** 316–346.

Huss G. R., Keil K., and Taylor G. J. (1981) The matrices of unequilibrated ordinary chondrites: implications for the origin and history of chondrites. *Geochim. Cosmochim. Acta* **45,** 3351.

Hutchison R., Alexander C. M. O., and Barber D. J. (1987) The Semarkona meteorite: First recorded occurrence of semctite in an ordinary chondrite, and its implications. *Geochim. Cosmochim. Acta* **51,** 1875–1882.

Jones R. H. (1990) Petrology and Mineralogy of type II chondrules in Semarkona (LL3.0): Origin of closed-system fractional crystallization, with evidence for supercooling. *Geochim. Cosmochim. Acta* **54,** 1785–1802.

Jones R. H. (1994) Petrology of FeO-poor, porphyritic pyroxene chondrules in the Semarkona chondrite. *Geochim. Cosmochim. Acta* **58,** 5325–5340.

Keil K. (1982) Composition and origin of chondritic breccia. In *Workshop on Lunar Breccias and Soils and Their Meteoritic Analogs* (ed. G. J. Taylor and L. L. Wilkening), pp. 65–83. Lunar Planet. Inst.

Kimura M. and Yagi K. (1980) Crystallization of chondrules in ordinary chondrites. *Geochim. Cosmochim. Acta* **44,** 589–602.

King E. A., ed. (1983) *Chondrules and Their Origins.* Lunar Planet. Inst. pp.

Kitamura M. and Tsuchiyama A. (1990) Comet-like grand-parent body of chondrites. *Proc. 15th Symp. Antartic Met.* **3,** 38–39.

Lewis R. D., Lofgren G. E., Franzen H. F., and Windom K. E. (1993) The effect of Na vapor on the Na content of chondrules. *Meteoritics* **28,** 622–628.

Lu J., Sears D. W. G., Keck B., Prinz M., Grossman J. N., and Clayton R. N. (1990) Semarkona type I chondrules compared with similar chondrules in other classes. *Lunar Planet. Sci.* **XXI,** 720–721.

Lux G., Keil K., and Taylor G. J. (1980) Metamorphism of the H-group chondrites: Implications from compositional and textural trends in chondrules. *Geochim. Cosmochim. Acta* **44,** 841–855.

Marshall D. J. (1988) *Cathodoluminescence of Geological Materials.* Unwin Hyman.

Matsunami S. et al. (1993) Thermoluminescence and compositional zoning in the mesostasis of a Semarkona group A1 chondrule and new insights into the chondrule-forming process. *Geochim. Cosmochim. Acta* **57,** 2101–2110.

McCoy T. J., Scott E. R. D., Jones R. H., Keil K., and Taylor G. J. (1991) Composition of chondrule silicates in LL3-5 chondrites and implications for their nebular history and parent body metamorphism. *Geochim. Cosmochim. Acta* **55,** 601–619.

McSween H. Y., Jr. (1977a) Carbonaceous chondrites of the Ornans types: A metamorphic sequence. *Geochim. Cosmochim. Acta* **41,** 477–491.

McSween H. Y., Jr. (1977b) Chemical and petrographic constraints on the origin of chondrules and inclusions in carbonaceous chondrites. *Geochim. Cosmochim. Acta* **41,** 1843–1860.

McSween H. Y., Jr. and Wilkening L. L. (1980) A note on the Allan Hills A77278 unequilibrated ordinary chondrite. *Meteoritics* **15,** 193–199.

McSween H. Y., Fronabarger A. K., and Driese S. G. (1983) Ferromagnesian chondrules in carbonaceous chondrites. In *Chondrules and Their Origins* (ed. E. A. King), pp. 195–210. Lunar Planet. Inst.

McSween H. Y., Jr., Sears D. W. G., and Dodd R. T. (1988) Thermal metamorphism. In *Meteorites and the Early Solar System* (ed. J. F. Kerridge and M. S. Matthews), pp. 102–113. Univ. Arizona Press.

Meeker G. P., Wasserburg G. J., and Armstrong J. T. (1983) Replacement textures in CAI and implications regarding planetary metamorphism. *Geochim. Cosmochim. Acta* **47,** 707–721.

Miyamoto M., McKay D. S., McKay G. A., and Duke M. C. (1986) Chemical zoning and homogenization of olivines in ordinary chondrites and implications for the thermal histories of chondrules. *J. Geophys. Res.* **91,** 12,804–12,816.

Morioka M. (1981) Cation diffusion in olivine. II. Ni-Mg, Mn-Mg, Mg, and Ca. *Geochim. Cosmochim. Acta* **45,** 1573–1580.

Muan A. and Osborn E. F. (1965) *Phase Equilibria Among Oxides in Steelmaking.* Addison-Wesley.

Radomsky P. M. and Hewins R. H. (1990) Formation conditions of pyroxene-olivine and magnesian-olivine chondrules. *Geochim. Cosmochim. Acta* **54,** 3475–3490.

Robie R. A., Hemingway B. S., and Fisher J. R. (1979) *Thermodynamic properties of minerals and related substances at 298.15 K and 1 Bar (10^5 Pascal) pressure and at high temperatures. Geological Survey Bulletin* **452.**

Roeder P. L. and Emslie R. F. (1970) Olivine-liquid equilibrium. *Contrib. Mineral. Petrol.* **29,** 275–289.

Scott E. R. D. (1984) Classification, metamorphism, and brecciation of type 3 chondrites from Antarctica. *Smithsonian Contrib. Earth Sci.* **26,** 73–94.

Scott E. R. D. and Taylor G. J. (1983) Chondrules and other components in C, O and E chondrites: Similarities in their properties and origins. *Proc. 14th Lunar Planet. Sci. Conf. Part I: J. Geophys. Res.* **88** (suppl.), B275–B286.

Scott E. R. D., Taylor G. J., and Keil K. (1982) Brecciated type 3 chondrites and their parent bodies. *Meteoritics* **17,** 278.

Sears D. W. G. and Hasan F. A. (1987) The type three ordinary chondrites: A review. *Surv. Geophys.* **9,** 43–97.

Sears D. W., Grossman J. N., Melcher C. L., Ross L. M., and Mills A. A. (1980) Measuring metamorphic history of unequilibrated ordinary chondrites. *Nature* **287,** 791–795.

Sears D. W. G., Hasan F. A., Batchelor J. D., and Lu Jie (1991) Chemical and physical studies of type 3 chondrites-XI: Metamorphism, pairing, and brecciation of ordinary chondrites. *Proc. Lunar Planet. Sci.* **21,** 495–512.

Sears D. W. G., Lu J., Benoit P. H., DeHart J. M., and Lofgren G. E. (1992) A compositional classification scheme for meteoritic chondrules. *Nature* **357,** 207–211.

Sears D. W. G. et al. (1995a) Metamorphism and aqueous alteration in low petrographic type ordinary chondrites. *Meteoritics* **30,** 169–181.

Sears D. W. G., Huang S., and Benoit P. H. (1995b) Chondrule formation, metamorphism, brecciation, an important new primary chondrule group, and the classification of chondrules. *Earth Planet. Sci. Lett.* **131,** 27–39.

Smith J. V. and Stenstrom R. C. (1965) Electron-excited luminescence as a petrologic tool. *J. Geology* **73,** 627–635.

Stöffler D., Keil K., and Scott E. R. D. (1991) Shock metamorphism of ordinary chondrites. *Geochim. Cosmochim. Acta* **55,** 3845–3867.

Tsuchiyama A., Nagahara H., and Kushiro I. (1981) Volatilization of sodium from silicate melt spheres and its application to the formation of chondrules. *Geochim. Cosmochim. Acta* **45,** 1357–1367.

Van Schmus W. R. and Wood J. A. (1967) A chemical-petrologic classification for the chondritic meteorites. *Geochim. Cosmochim. Acta* **31,** 747–765.

Wood J. A. (1985) Meteoritic constraints on processes in the solar nebula. In *Protostars and Planets II* (ed. D. C. Black and M. S. Matthews), pp. 682–702. Univ. Arizona Press.

Wood J. A., Hashimoto A., and Holmberg B. B. (1989) Chondrules as near-equilibrium assemblages that formed in fractionated systems. *Lunar Planet. Sci.* **XX,** 1215–1216.

Yu Y. and Hewins R. H. (1994) Retention of sodium under transient heating conditions for the chondrule forming environment. *Lunar Planet. Sci.* **XXV,** 1535–1536.